Molecular Plant Pathology

MOLECULAR PLANT PATHOLOGY (2013) **14**(5), 470–482 DOI: 10.1111/mpp.12020

The actin-regulating kinase homologue MoArk1 plays a pleiotropic function in *Magnaporthe oryzae*

JIAMEI WANG[1,2], YAN DU[1,2], HAIFENG ZHANG[1,2], CHEN ZHOU[1,2], ZHONGQIANG QI[1,2], XIAOBO ZHENG[1,2], PING WANG[3] AND ZHENGGUANG ZHANG[1,2,*]

[1]*Department of Plant Pathology, College of Plant Protection, Nanjing Agricultural University, Nanjing 210095, China*
[2]*Key Laboratory of Integrated Management of Crop Diseases and Pests, Ministry of Education, Nanjing 210095, China*
[3]*Department of Pediatrics and the Research Institute for Children, Louisiana State University Health Sciences Center, New Orleans, LA 70118, USA*

SUMMARY

Endocytosis is an essential cellular process in eukaryotic cells that involves concordant functions of clathrin and adaptor proteins, various protein and lipid kinases, phosphatases and the actin cytoskeleton. In *Saccharomyces cerevisiae*, Ark1p is a member of the serine/threonine protein kinase (SPK) family that affects profoundly the organization of the cortical actin cytoskeleton. To study the function of MoArk1, an Ark1p homologue identified in *Magnaporthe oryzae*, we disrupted the *MoARK1* gene and characterized the Δ*Moark1* mutant strain. The Δ*Moark1* mutant exhibited various defects ranging from mycelial growth and conidial formation to appressorium-mediated host infection. The Δ*Moark1* mutant also exhibited decreased appressorium turgor pressure and attenuated virulence on rice and barley. In addition, the Δ*Moark1* mutant displayed defects in endocytosis and formation of the Spitzenkörper, and was hyposensitive to exogenous oxidative stress. Moreover, a MoArk1-green fluorescent protein (MoArk1-GFP) fusion protein showed an actin-like localization pattern by localizing to the apical regions of hyphae. This pattern of localization appeared to be regulated by the *N*-ethylmaleimide-sensitive factor attachment protein receptor (SNARE) proteins MoSec22 and MoVam7. Finally, detailed analysis revealed that the proline-rich region within the MoArk1 serine/threonine kinase (S_TKc) domain was critical for endocytosis, subcellular localization and pathogenicity. These results collectively suggest that MoArk1 exhibits conserved functions in endocytosis and actin cytoskeleton organization, which may underlie growth, cell wall integrity and virulence of the fungus.

INTRODUCTION

Eukaryotic cells internalize macromolecules and other materials from the extracellular medium through the conserved process of endocytosis. Consequentially, endocytosis serves multiple functions, including the recycling of membrane proteins and lipids, internalization of membrane proteins and lipids for degradation and internalization of signalling molecules (D'Hondt *et al*., 2000; Emans *et al*., 2002). In the budding yeast *Saccharomyces cerevisiae*, the availability of the fluorescent dye FM4-64 and Ste2p and Ste3p pheromone receptors has allowed for the identification of the endocytic pathway (Toret and Drubin, 2006). Many features of the yeast endocytic pathway are also surprisingly conserved in mammalian systems (Davis *et al*., 1993; Raths *et al*., 1993). In yeasts and other fungi, either pathogenic or saprophytic, endocytosis and intracellular transport events are important for cellular functions, including polarity establishment, hyphal growth and/or virulence (Atkinson *et al*., 2002; Dou *et al*., 2011; Read and Kalkman, 2003; Shaw *et al*., 2011; Song *et al*., 2010; Wang and Shen, 2011). Numerous studies have examined the important roles of specific endocytic components, such as *Aspergillus oryzae* End4/Sla2, *Fusarium graminearum* End1, *Ustilago maydis* Yup1 and mammalian cyclin-G-associated kinase (GAK) and adaptor-associated kinase 1 (AAK1) (Fuchs *et al*., 2006; Higuchi *et al*., 2009; Kim *et al*., 2009; Smythe and Ayscough, 2003). In mammalian cells, members of the Ark/Prk family of kinases, including GAK and AAK1, are important for endocytosis (Smythe and Ayscough, 2003). The roles of endocytic transport in the growth and pathogenicity of *U. maydis* have also been subject to in-depth discussions (Fuchs and Steinberg, 2005; Steinberg, 2007). The importance of endocytosis as a physiological pathway and the molecular mechanism of endocytosis have also been reported. For example, *Aspergillus nidulans* actin and myosin are important factors in endocytosis and polarized cell growth (Kaksonen *et al*., 2006). In addition, phosphorylation of *A. nidulans* MyoA regulates events in the endocytic pathway, such as membrane internalization (Hervas-Aguilar and Penalva, 2010; Idrissi *et al*., 2008). These reports further highlight that the endocytic pathway is important for engaging in normal physiological functions in filamentous fungi, similar to other well-defined eukaryotic cells.

In the rice blast fungus *Magnaporthe oryzae*, infection occurs by conidia that are normally composed of three cells. The germination of conidia involves the production of a germ tube from one or more of these cells (Howard and Valent, 1996).

*Correspondence: Email: zhgzhang@njau.edu.cn

Endocytosis is thought to be important for conidial cells to detect certain external signals, and plays a crucial role in various aspects of hyphal tip growth (Fischer-Parton *et al*., 2000). Successful detection for the incorporation of FM4-64 into the Spitzenkörper body identified this organelle as being involved in endocytic membrane trafficking (Fischer-Parton *et al*., 2000; Harris *et al*., 2005; Verdin *et al*., 2009). Despite these findings, the physiological importance and molecular process of the endocytic process in filamentous fungi remain largely unaddressed, and little is known regarding the exocytotic transport of enzymes and other cell wall lytic materials in host tissue-invading processes (Gow *et al*., 2002). Previously, we have characterized MoSec22 and MoVam7 as two members of the secretory soluble *N*-ethylmaleimide-sensitive factor attachment protein receptor (SNARE) complex in *M. oryzae*, and have found that they play important roles in membrane trafficking, as well as in cellular growth, stress tolerance and pathogenicity (Dou *et al*., 2011; Song *et al*., 2010). SNARE proteins are a family of conserved proteins involved in the intracellular transport of membrane-coated cargo from one subcellular compartment to another (Pelham, 1999). As a part of our continuing research efforts to examine the roles of membrane trafficking in fungal pathogenesis, we analysed the physiological significance of MoArk1, the *S. cerevisiae* actin-regulating kinase 1 (Ark1) homologue in *M. oryzae*. In the present study, we demonstrated that MoArk1 regulates endocytosis and is required for conidial development, stress resistance, membrane trafficking and pathogenicity.

RESULTS

Identification and characterization of *MoARK1*

Examination of the *M. oryzae* genome database at the Broad Institute (http://www.broad.mit.edu/annotation/genome/magnaporthe_grisea/Home.html) revealed that MGG_11326.6 shares high amino acid sequence homology to *S. cerevisiae* Ark1p (ScArk1p), and we thus named it MoArk1. MoArk1 consists of 1021 amino acids and appears to be encoded by a single-copy gene. Similar to ScArk1p, MoArk1 contains a putative serine/threonine kinase (S_TKc) domain in its N-terminus, and three phosphorylation sites and a conserved proline-rich motif RPTAPPKP in its C-terminus (Fig. S1A, see Supporting Information). MoArk1 shares 56% amino acid sequence identity with ScArk1p and 58% with the *N. crassa* Ark1 homologue. In contrast, MoArk1 is less similar to human Gak1 (17%) and *Drosophila melanogaster* auxilin (15%) (Fig. S1B). To address the function of MoArk1 in *M. oryzae*, the targeted gene deletion vector pMD-*MoARK1*KO was introduced into the wild-type strain (Fig. S2A, see Supporting Information), and two Δ*Moark1* mutants were confirmed by reverse transcription-polymerase chain reaction (RT-PCR) and Southern blot analysis (Fig. S2B, C).

MoARK1 affects endocytosis and formation of the Spitzenkörper body

Because ScArk1p is involved in endocytosis and the actin cytoskeleton, we first evaluated whether the loss of *MoARK1* also resulted in defects in endocytosis and intracellular transport. We performed FM4-64 staining to examine vacuolar membrane internalization. In wild-type cells, visible internal staining suggested rapid uptake of the FM4-64 dye and functional endocytosis. In these cells, FM4-64 was internalized within 15 min of incubation, resulting in various bright ring-like stained structures representing endosomes and vesicles. In contrast, no definitive staining pattern was observed in the hyphal cell of the Δ*Moark1* mutant, either at the plasma membrane or in the cytosol, up to 30–45 min after exposure to the dye. Reintroduction of the *MoARK1* gene to the Δ*Moark1* mutant restored the staining pattern (Fig. 1A). These results indicate that the Δ*Moark1* mutant is altered in endocytosis.

The Spitzenkörper body is a dynamic structure present at the tips of hyphal cells with a single highly polarized growth site. It is closely associated with cellular morphogenesis and polar growth and is only present at actively growing sites (Virag and Harris, 2006). Recent studies have suggested that the Spitzenkörper is involved in both exocytosis and endocytosis. To examine whether the endocytosis defect of the Δ*Moark1* mutation also affected Spitzenkörper formation, we observed Spitzenkörper formation using FM4-64 staining. The Spitzenkörper was readily visible

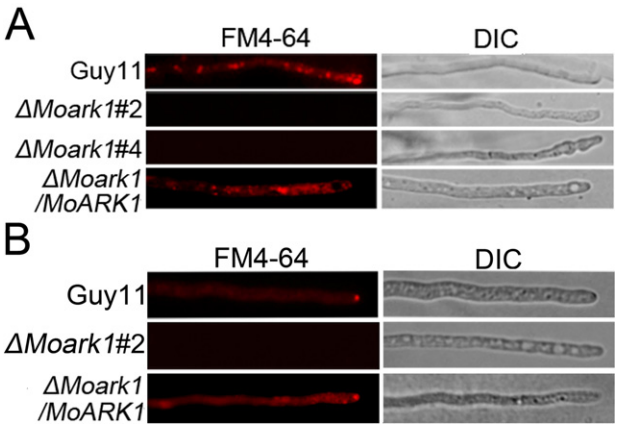

Fig. 1 MoArk1 has a role in the formation of the Spitzenkörper and endocytosis. (A) FM4-64 staining revealed that the Δ*Moark1* mutant was defective in endocytosis. Strains were grown for 2 days on complete medium (CM)-overlaid microscope slides before the addition of FM4-64 and photographs were taken after 15 min of exposure to FM4-64. Camera exposure is indicated in seconds (800 ms). (B) The wild-type and complemented strains showed the presence of an intact Spitzenkörper at the tips of the hyphae, which was missing in the Δ*Moark1* mutants after exposure to FM4-64 staining for 15 min. Strains were grown for 2 days on CM-overlaid microscope slides before staining. DIC, differential interference contrast image.

within 15 min of incubation in the wild-type strain, but not in the Δ*Moark1* mutants, even after extended incubation (Fig. 1B), suggesting that disruption of *MoARK1* results in defects in Spitzenkörper formation.

Growth defects of Δ*Moark1* mutants on various media

Given that ScArk1p was identified as relevant to the growth characteristics of the yeast cell (Smythe and Ayscough, 2003), we investigated whether MoArk1 had a similar role. After incubation at 28 °C for 7 days in the dark, the Δ*Moark1* mutant showed reduced growth rates, sparse aerial mycelia and abnormal pigmentation on various media, including complete medium (CM), oatmeal agar medium (OM), straw decoction and corn agar (SDC) and V8 (Fig. 2A). This suggests that the loss of MoArk1 may reduce the fitness of the Δ*Moark1* mutant. The dry weight of the mycelium, which was incubated in CM for 48 h, was reduced significantly by >30% when compared with the wild-type, indicating that MoArk1 is important for growth (Fig. 2B). To determine whether the deletion of MoArk1 affected growth on complex media, wild-type Guy11, the Δ*Moark1* mutant and complemented strains were cultured on GMM [1% glucose minimal medium: 0.52 g/L KCl, 0.52 g/L $MgSO_4 \cdot 7H_2O$, 1.52 g/L KH_2PO_4, 10 g/L glucose, 0.001% (W/V) thiamine and 0.1% (W/V) trace elements] or FMM [1% fructose minimal medium: 0.52 g/L KCl, 0.52 g/L $MgSO_4 \cdot 7H_2O$, 1.52 g/L KH_2PO_4, 10 g/L fructose, 0.001% (W/V) thiamine and 0.1% (W/V) trace elements] containing different carbon and nitrogen sources, such as vitamins (VA), casamino acids (CA), peptone (PE), yeast extract (YE), yeast nitrogen base without amino acids (YN-AA), $NaNO_3$ and $(NH_4)_2SO_4$. The results showed that the Δ*Moark1* mutant grew much more slowly than the wild-type and

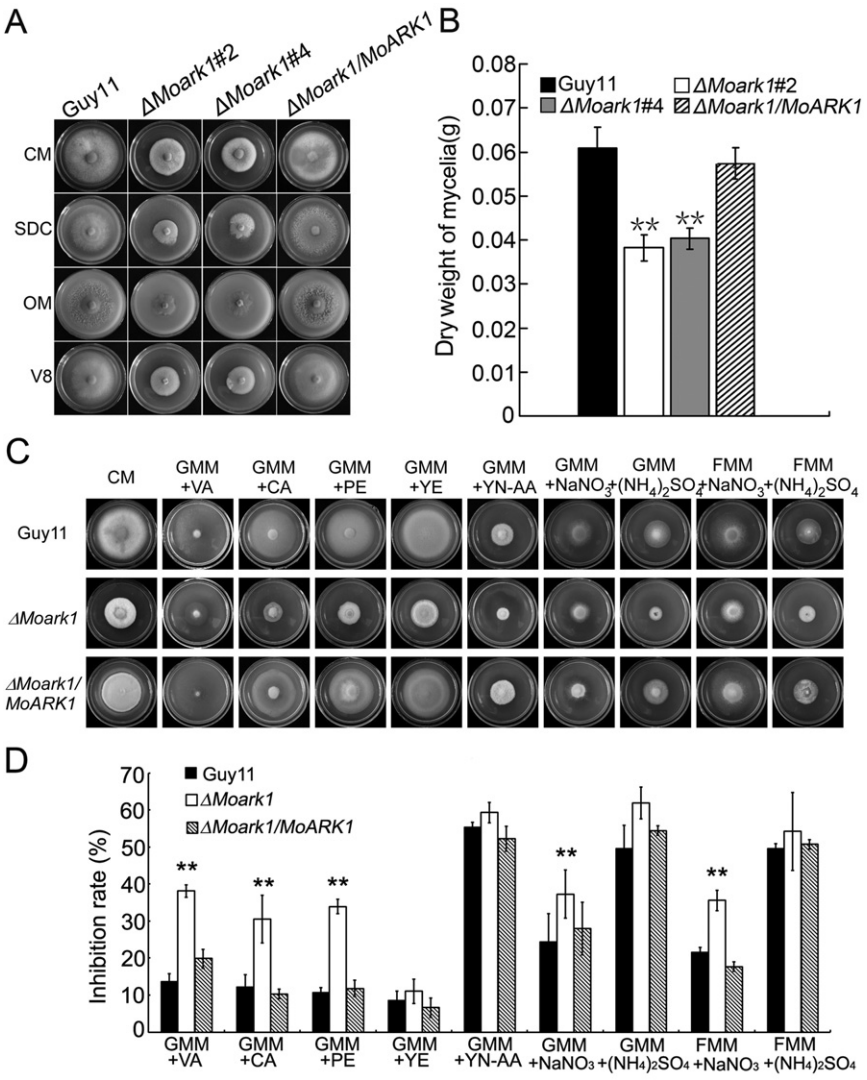

Fig. 2 MoArk1 is required for normal mycelial growth on various media. (A) The Δ*Moark1* mutants displayed reduced mycelial growth on complete medium (CM), straw decoction and corn agar (SDC), oatmeal agar (OM) and V8 medium following incubation of plates at 28 °C for 7 days in the dark. (B) Mycelium dry weight assessment of cultures of Δ*Moark1* mutants, wild-type and complemented strains (Δ*Moark1/MoARK1*). (C) Supplements, such as vitamins (VA), casamino acids (CA), peptone (PE), yeast extract (YE) and yeast nitrogen base without amino acids (YN-AA), were added in the same amounts to GMM [1% glucose minimal medium: 0.52 g/L KCl, 0.52 g/L $MgSO_4 \cdot 7H_2O$, 1.52 g/L KH_2PO_4, 10 g/L glucose, 0.001% (W/V) thiamine and 0.1% (W/V) trace elements; containing 10 mM NH_4^+] to determine what component(s) of CM remediated Δ*Moark1* growth. In addition, 100 mM $NaNO_3$ or 50 mM $(NH_4)_2SO_4$ was added to 1% glucose or 1% fructose to compare the different monosaccharide absorption differences. (D) Statistical analyses of the inhibition rate of wild-type Guy11, Δ*Moark1* mutant and the complemented strains on different sole nitrogen and carbon sources. Error bars represent the standard deviations and asterisks denote statistical significances ($P < 0.01$).

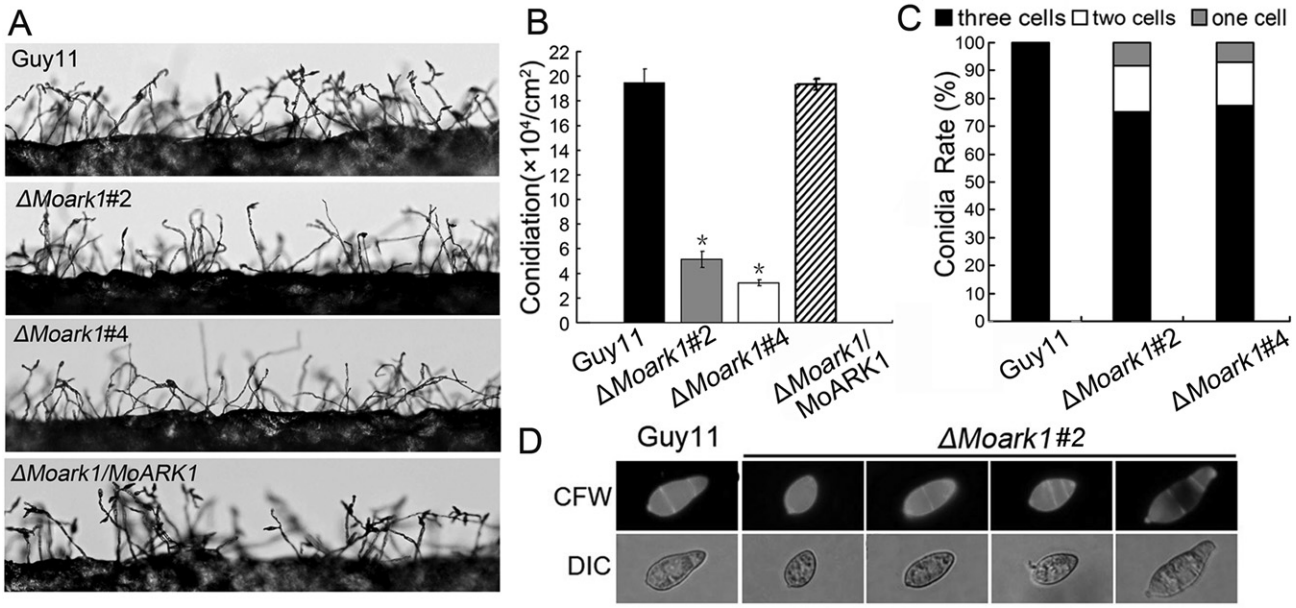

Fig. 3 The Δ*Moark1* deletion mutants show abnormal conidial morphology and reduced conidiation. (A) Development of conidia on conidiophores is affected by *MoARK1* disruption. Strains grown on straw decoction and corn agar (SDC) medium for 7 days were examined by light microscopy. (B) Statistical analysis of conidia production. The conidia produced by the wild-type strain (Guy11), mutants and complemented strains grown on SDC medium for 10 days were collected, counted and analysed by Duncan analysis ($P < 0.01$). Asterisks indicate significant differences among Guy11, the Δ*Moark1* mutant and complemented strains. Three independent experiments yielded similar results. Error bars represent standard deviation ($n = 3$). (C) The percentage of each type of abnormal conidia ($n = 100$). Three independent experiments were performed and similar results were obtained. (D) Conidia shape comparison. The conidia were stained with calcofluor white and photographed.

complemented strains on GMM + VA, GMM + CA, GMM + PE, GMM + $NaNO_3$ and FMM + $NaNO_3$ media (Fig. 2C, D). In contrast, no significant difference was observed between the wild-type and Δ*Moark1* mutant on GMM + YE, GMM + YE-AA and FMM + $(NH_4)_2SO_4$ media (Fig. 2C, D). These results indicate that MoArk1 plays a crucial role in nutrient uptake.

MoArk1 disruption results in a reduction in conidia formation and abnormal conidium morphology

Conidia play an important role in the disease cycle of rice blast (Lee *et al*., 2006). To examine the role of MoArk1 in conidium production, conidiation of the wild-type strain (Guy11), Δ*Moark1* mutants (#2 and #4) and the complemented strain (Δ*Moark1/MoARK1*) from 7-day-old SDC culture was examined. Conidia formation was reduced by approximately two- to three-fold in the Δ*Moark1* mutants compared with the wild-type and complemented strains (Fig. 3A–C). Some of the conidia formed by Δ*Moark1* mutants also showed abnormal morphology. Calcofluor white (CFW) staining showed that 30% of the mutant conidia had only one or two cells, in contrast with the mostly (~95%) three-celled conidia of the wild-type (Fig. 3D). Surprisingly, we found that Δ*Moark1* mutants showed no obvious defect in conidium germination and appressorium formation. These results suggest that the loss of MoArk1 affects conidiogenesis and conidial morphology.

MoArk1 directly or indirectly contributes to the pathogenicity of *M. oryzae*

To determine whether MoArk1 is involved in pathogenesis, conidial suspensions (5×10^4 spores/mL) from the wild-type, two independently generated Δ*Moark1* mutants and complemented strains were sprayed onto susceptible rice seedlings (CO-39 cv. *oryzae*) and detached barley leaves. After 7 days, the Δ*Moark1* mutants still caused disease lesions, but a significant reduction in lesion number was found compared with those produced by the controls (Fig. 4A). Disease on rice was also quantified using a 'lesion-type' scoring assay (Valent *et al*., 1991), which showed that, although lesion types 1–3 were produced by both the Δ*Moark1* mutants and wild-type, lesion types 4 and 5 (severe, coalescing) were not produced by the mutant (Fig. 4B). On detached barley leaves, which were inoculated with three different concentrations of conidial suspension (1×10^5, 1×10^4 and 1×10^3 spores/mL), lesions produced by the Δ*Moark1* mutants were less severe (Fig. 4C). Thus, a loss of MoArk1 function reduces the colonization of leaves by the rice blast fungus.

Δ*Moark1* mutants are altered in the generation of appressorium turgor pressure

To penetrate the rice leaf cuticle and cause infection, a high appressorium internal turgor pressure is required (Talbot and

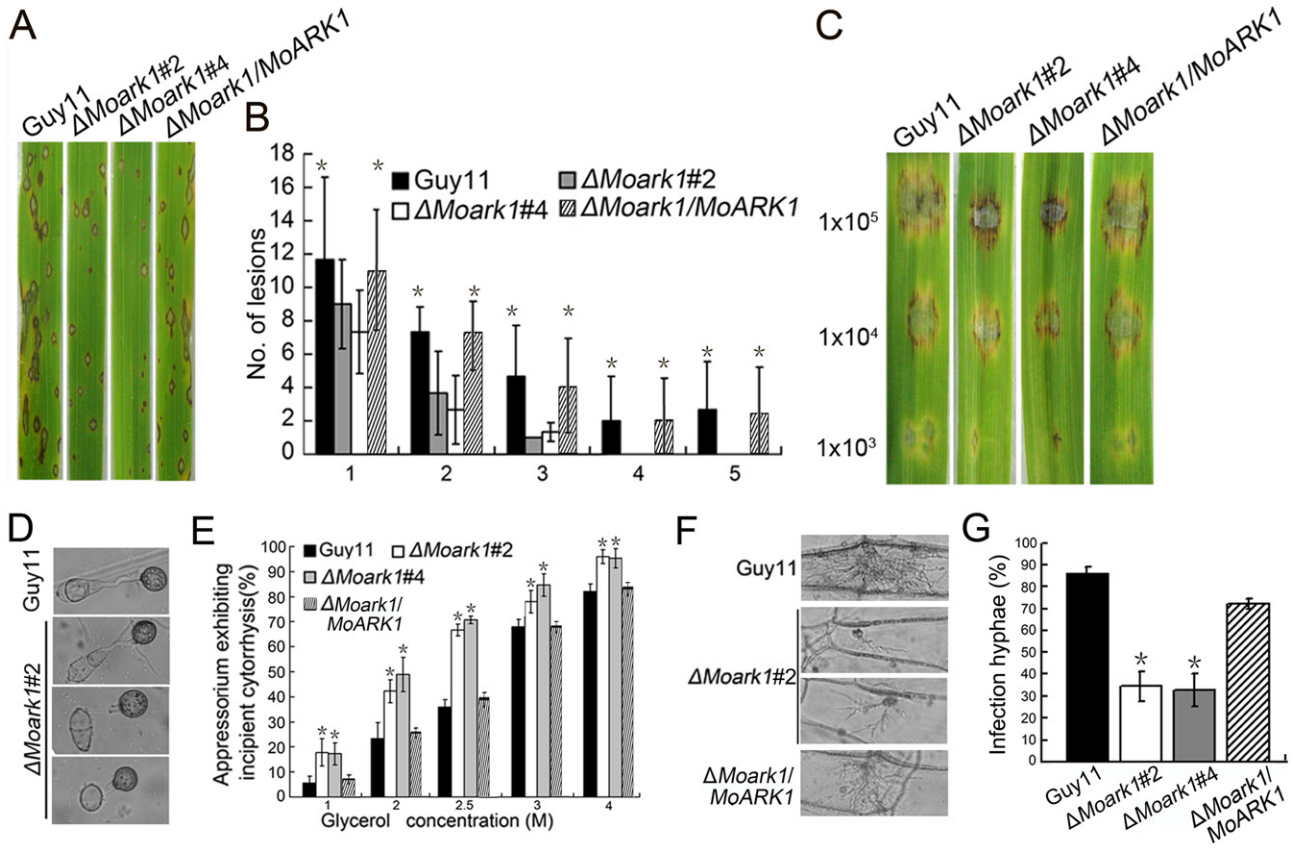

Fig. 4 *MoARK1* deletion attenuated pathogenicity. (A) The *MoARK1* deletion attenuated pathogenicity on rice leaves. (B) Quantification of lesion type (0, no lesion; 1, pinhead-sized brown specks; 2, 1.5-mm brown spots; 3, 2–3-mm grey spots with brown margins; 4, many elliptical grey spots longer than 3 mm; 5, coalesced lesions infecting 50% or more of the leaf area) reveals no difference in lesion types 1–3; however, the Δ*Moark1* mutants do not make any lesions of types 4 and 5. Lesions were photographed and measured or scored at 7 days post-inoculation (dpi) and experiments were repeated twice with similar results. $n = 35$ for each mutant. (C) Conidia containing different concentrations of Δ*Moark1* mutants were drop inoculated onto barley and show a virulence defect compared with the wild-type strain (Guy11) and complemented strains, as manifested by smaller lesions at 5 dpi. (D) Appressoria formation is altered in the Δ*Moark1* mutant. (E) Collapsed appressoria were observed in the wild-type Guy11, Δ*Moark1* mutant and complemented strains. For each glycerol concentration, at least 100 appressoria were observed and the numbers of collapsed appressoria were counted. (F) The Δ*Moark1* mutants exhibited reduced host penetration on onion epidermis after 48 h in contrast with control strains. (G) Quantification of hyphae infection on onion epidermis after 48 h. Three independent biological experiments yielded similar results. Error bars represent standard deviation, and asterisks represent significant difference between Guy11 and mutants ($P < 0.01$).

Foster, 2001; Thines *et al*., 2000). Appressorium turgor can be measured using an incipient cytorrhysis assay, which uses hyperosmotic concentrations of a solute to collapse the appressoria (DeJong *et al*., 1997). As appressorial formation appears to be normal in the Δ*Moark1* mutants (Fig. 4D), we hypothesized that the reduced pathogenicity may be a result of a defect in appressorium turgor pressure. The appressoria of the Δ*Moark1* mutants showed an increased collapse rate even in 1 M glycerol solution (Fig. 4E), validating our hypothesis. We further inoculated the conidial suspensions onto onion epidermis and found that only a small number of appressoria were developed after 48 h (approximately 30%, compared with 95% in the wild-type) (Fig. 4F). The wild-type strain exhibited an approximately 85% penetration rate, whereas the penetration rate of the Δ*Moark1* mutants was only 30%. The percentage of infectious hyphae in the wild-type was also distinct from that of the Δ*Moark1* mutant (Fig. 4G). These results indicate that the reduced pathogenicity of the Δ*Moark1* mutant is caused, at least in part, by defects in appressorium turgor pressure and subsequent host penetration.

Δ*Moark1* mutants are defective in infectious hyphal growth on the plant

To further explore the reasons why Δ*Moark1* mutants show reduced virulence on host plants, we examined the invasive hyphal growth on both barley leaves and rice leaf sheaths. After incubation with the spore suspensions for 48 h, four types (type 1, no penetration; type 2, with penetration peg; type 3, with a single invasive hypha; type 4, with extensive hyphal growth) of invasive hyphae were observed in barley tissues (Fig. 5A). In the wild-type

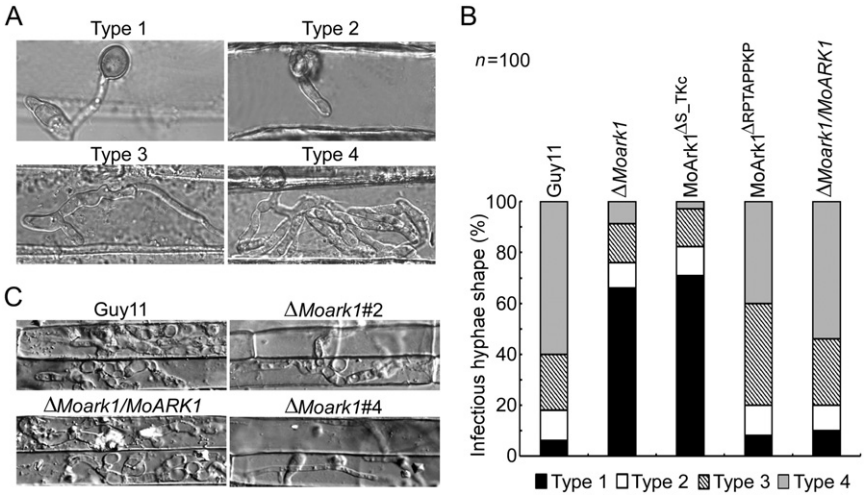

Fig. 5 Colonization of Δ*Moark1* mutant on plants. (A) Close observation of infectious growth on barley. Excised barley leaves from 7-day-old barley seedlings were inoculated with conidial suspension (1×10^4 spores/mL of each strain). Infectious growth was observed at 24 h post-inoculation (hpi). (B) Statistical analysis for each type of infectious hyphal shape, for each tested strain; 100 infecting hyphae ($n = 100$) were counted per replicate and the experiment was repeated three times. (C) Excised rice sheath from 4-week-old rice seedlings was inoculated with conidial suspension (1×10^4 spores/mL of each strain). Infectious growth was observed at 48 hpi.

Guy11 and the complemented strains, 60% of cells showed type 4 and 18% showed type 1 and type 2 invasive hyphal growth. In contrast, less than 10% of cells showed type 4 and more than 80% showed type 1 and type 2 invasive hyphal growth in the Δ*Moark1* mutants. In addition, in the proline-rich domain deletion mutant, 40% of cells showed type 4 and 20% showed type 1 and type 2 (Fig. 5A, B). A similar result was observed in rice leaf sheaths, with the wild-type Guy11 and complemented strains displaying faster hyphal growth extension to neighbouring cells and the Δ*Moark1* mutants showing lower hyphal growth limited to one cell (Fig. 5C). These results indicate that MoArk1 plays an important role in infectious hyphal growth and plant colonization.

Δ*Moark1* mutants are less sensitive to salt and osmotic stress

To investigate the role of MoArk1 in stress responses, such as sensitivity to salt and osmotic adaptation, the wild-type Guy11, Δ*Moark1* and complemented strains were exposed to various conditions, including ion stress (Na^+ and K^+) and osmotic stress (sorbitol). The Δ*Moark1* mutant exposed to 0.7 M NaCl, 1 M sorbitol and 1.2 M KCl showed 20%, 8% and 45% lower growth inhibition, respectively, than the wild-type strain (Fig. S3A, B, see Supporting Information). This demonstrates that the lack of MoArk1 affects salt and osmotic adaptation.

Cell wall integrity is altered in the Δ*Moark1* mutants

As the fungal cell wall plays an essential role in maintaining hyphal morphology and adaptation to the environment, the structural integrity of the Δ*Moark1* mutant cell wall and membrane was examined. Mycelial growth was measured on CM containing various concentrations of cell wall stressors, including CFW, sodium dodecylsulphate (SDS) and Congo Red (CR). In growth assays with three different concentrations of CFW, the Δ*Moark1* mutant showed slight resistance to CFW with an average 8%, 10% and 12% lower growth inhibition than the wild-type and complemented strains, which were 30%, 40% and 50%, respectively (Fig. S4A, B, see Supporting Information). The responses to SDS and CR were slightly different. At lower concentrations, the Δ*Moark1* mutants showed sensitivity to these stress inducers, but, at higher concentrations, the mutants showed more resistance (Fig. S4C–E). The results were largely supportive of our hypothesis that MoArk1 plays a role in cell wall integrity.

Deletion of *MoARK1* alters chitin distribution

Previous studies have shown that Δ*Movam7* and Δ*Mosec22* mutants exhibit abnormal chitin distributions, which are not restricted to growing apices, but also occur on lateral walls along hyphal axes. In the wild-type *M. oryzae* strain, CFW fluorescence was mostly distributed at the septa and tips where chitin, one of the main components of the fungal cell wall, is actively synthesized. In the Δ*Moark1* mutants, patches of bright fluorescence were observed on the lateral wall of hyphae in addition to septa and hyphal tips (Fig. 6A). This abnormal distribution of cell wall components was restored by the reintroduction of wild-type MoArk1 (Fig. 6A). As a result of continuous tip elongation in filamentous fungi, these organisms may need to recycle certain components, such as cell wall-building enzymes, to the tip region. As CFW intercalates with nascent chitin chains, this result suggests that the altered distribution of chitin on the Δ*Moark1* mutant cell wall could be caused by aberrant cell wall synthesis activities.

In addition, we examined the effects of lytic enzymes (10 mg/mL lysing enzymes) on the Δ*Moark1* mutant. More protoplasts were found in the Δ*Moark1* mutant than in the controls after treatment for 60 and 90 min (Fig. 6B). When observed at 60 min, the Δ*Moark1* mutant showed a greater number of protoplasts and almost no mycelial fragments were observed, in contrast with the wild-type, where mycelial fragments were still found (Fig. 6C).

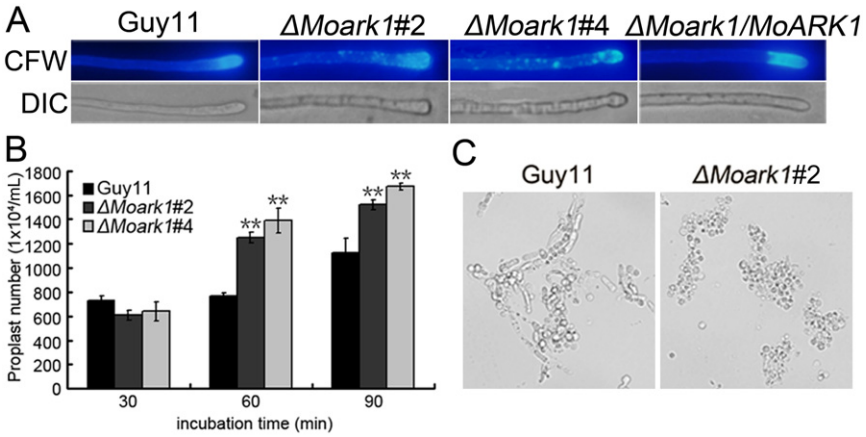

Fig. 6 Mycelial calcofluor white (CFW) staining and protoplast release assay. (A) Disruption of *MoARK1* altered the distribution of chitin on the cell wall. Wild-type and mutant hyphae were stained with 10 μg/mL CFW for 5 min without light before being photographed. The experiment was repeated three times with triplicates, and displayed the same results. DIC, differential interference contrast image. (B) Protoplast release assay of Guy11 and Δ*Moark1* mutants. Asterisks indicate a significant difference between the mutants and wild-type strain at $P < 0.01$, according to Duncan's range test. (C) Light microscopic examination of protoplast release after 40 min.

Δ*Moark1* mutants are less sensitive to oxidative stress and exhibit higher extracellular peroxidase activities

In fungi, secreted peroxidases are regarded as an important component to help pathogens detoxify host-derived reactive oxygen species during plant–microbe interactions (Guo *et al*., 2010). To investigate whether MoArk1 was involved in the oxidative stress response, wild-type Guy11, Δ*Moark1* mutants and the complemented strains were exposed to hydrogen peroxide (H_2O_2). The mycelial growth of the Δ*Moark1* mutants was affected slightly (Fig. S5A, see Supporting Information). Exposure to 2.5 and 5 mM H_2O_2 led to an average 5% (2.5 mM) and 13% (5 mM) decrease, respectively, in growth inhibition compared with the wild-type strain (Fig. S5B).

We next evaluated the influence of H_2O_2 on CR degradation, as indicated by the presence of discolored halos surrounding the colony. Discolored halos were observed in the Δ*Moark1* mutants and the control strain (Fig. S5C). The discoloration appeared to be more solid than in the wild-type, suggesting that MoArk1 might also affect peroxidase activity. Indeed, enzyme activity assays using extracellular culture filtrates and 2,2′-Azino-bis(3-ethyl benzothiazoline-6-sulfonic acid) diammonium salt (ABTS) as a substrate revealed that the Δ*Moark1* mutant exhibited stronger peroxidase activity (Fig. S5D). We further examined the transcriptional levels of four peroxidase-encoding genes, all of which possess a signal peptide (MGG_04545.6, MGG_13291.6, MGG_08730.6 and MGG_07790.6). We found that the expression levels for three of these genes were increased in the Δ*Moark1* mutants (Fig. S5D). These data suggest that MoArk1 is involved in controlling extracellular peroxidase activities by negative feedback regulation.

A proline-rich motif is responsible for the subcellular localization of MoArk1

In *S. cerevisiae*, Ark1p was found to affect the organization of the cortical actin cytoskeleton. Actin plays multiple complex roles in cell growth and cell shape (Heath *et al*., 2003). Recently, actin patches, which represent sites of endocytosis, have been demonstrated to be present in a subapical collar at the growing tips of hyphae and germ tubes of filamentous fungi. This zone of endocytosis is now known to be necessary for filamentous growth to proceed (Kaksonen *et al*., 2003). A ScArk1p-green fluorescent protein (ScArk1p-GFP) fusion protein was visible in the cortical patch structure with a very similar appearance and behaviour to actin patches. When GFP and actin were both visualized by indirect immunofluorescence, they were found to co-localize in patches at the cell cortex (Smythe and Ayscough, 2003). To investigate whether MoArk1 exhibits the actin-like distribution pattern, we detected the subcellular localization of MoArk1 using a *MoARK1*-GFP fusion protein. In Δ*Moark1* expressing MoArk1-GFP, fluorescence was detected mainly in vacuole-like patches in vegetative hyphal tips. Meanwhile, the hyphae were stained with rhodamine–phalloidin which binds actin after 48 h of static culture, which showed red fluorescence co-localizing with MoArk1-GFP fluorescence (Fig. 7A). During appressoria development, fluorescent signals were also detected at the periphery of appressoria and in vacuoles. In mature appressoria (24 h), GFP signals were mainly localized to globular structures at the base of mature appressoria (Fig. 7B).

Proline-rich (KPxPPPKP) regions are known to mediate protein–protein interactions and can be bound by Src-homology (SH3) domains (Cope *et al*., 1999). Several interactions involving proline-rich motifs and SH3 domains are found among proteins in yeast cortical actin patches. MoArk1 may also participate in such associations. We generated the *MoARK1*$^{\Delta RPTAPPKP}$-GFP construct and transformed it into Δ*Moark1* protoplasts. In the resulting transformants, the GFP fluorescence was weaker and the Ark1 localization pattern was not observed in hyphae and mature appressoria, compared with the *MoARK1*-GFP transformants (Fig. 7C, D). We also examined the GFP signal during infection. The *MoARK1*-GFP transformant showed an actin-like localization pattern in the plant cells. However, only dispersed GFP signal was observed in the *MoARK1*$^{\Delta RPTAPPKP}$-GFP and *MoARK1*$^{\Delta S\_TKc}$-GFP

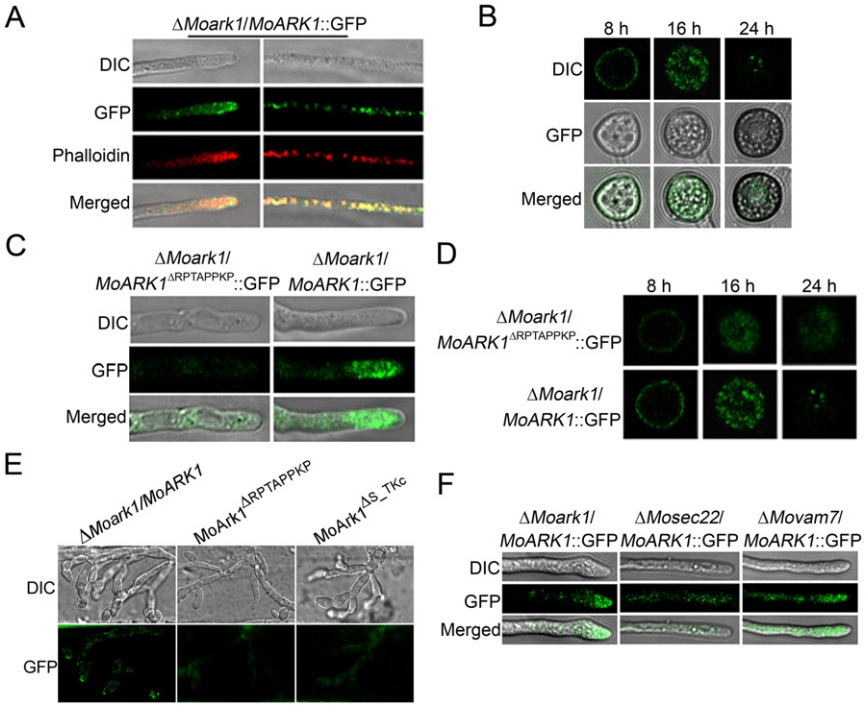

Fig. 7 Cellular localization of MoArk1-green fluorescent protein (MoArk1-GFP) and MoArk1$^{\Delta RPTAPPKP}$-GFP. (A) Vegetative hyphal tips were observed under laser scanning confocal microscopy. The hyphae were stained with the actin dye rhodamine-phalloidin after 48 h of static culture. DIC, differential interference contrast image. (B) Δ*Moark1*/MoArk1-GFP fluorescence observation during appressoria formation process after 8, 16 and 24 h under laser scanning confocal microscopy. (C) Vegetative hyphal tips of Δ*Moark1*/MoArk1$^{\Delta RPTAPPKP}$-GFP were observed under laser scanning confocal microscopy. (D) Δ*Moark1*/MoArk1$^{\Delta RPTAPPKP}$-GFP fluorescence observation during appressoria formation process after 8, 16 and 24 h under laser scanning confocal microscopy. (E) Invasive hyphae produced by the *MoARK1*-GFP, *MoARK1*$^{\Delta RPTAPPKP}$-GFP and *MoARK1*$^{\Delta S_TKc}$-GFP transformants in onion epidermal cells at 24 hpi. (F) Vegetative hyphal tips of Δ*Moark1*/*MoARK1*, Δ*Mosec22*/*MoARK1* and Δ*Movam7*/*MoARK1* under laser scanning confocal microscopy.

transformants (Fig. 7E). The above results indicate that the proline-rich region is responsible for the subcellular localization of MoArk1, as well as pathogenicity.

MoArk1 subcellular localization involves functions of SNARE proteins MoVam7 and MoSec22

SNARE proteins ensure the specific recognition and transportation of vesicles and target membrane-mediated fusions (Fukuda *et al*., 2000). Our previous studies identified two SNARE proteins, MoVam7 and MoSec22, which are involved in cell membrane transport and endocytosis (Dou *et al*., 2011; Song *et al*., 2010). To determine whether MoVam7 and MoSec22 were involved in the subcellular localization of MoArk1, we transformed *MoARK1*-GFP into the Δ*Mosec22* and Δ*Movam7* mutants. We found that GFP fluorescence was clustered at the hyphal tip in the Δ*Moark1*/*MoARK1* complemented strain. In contrast, the fluorescence was primarily internal in the hyphae of Δ*Mosec22*/*MoARK1*-GFP and Δ*Movam7*/*MoARK1*-GFP mutants (Fig. 7F). This suggests that the lack of MoSec22 and MoVam7 disturbs vesicle transport, which affects the normal localization of MoArk1.

Functional characterization of different domains of *MoARK1*

MoARK1 has an S/TKc domain and a RPTAPPKP motif, similar to ScArk1p. We also generated mutant alleles of *MoARK1*-GFP (Fig. 8A). Transformants expressing the MoArk$^{\Delta S_TKc}$-GFP showed similar phenotypes to Δ*Moark1*, which exhibited reduction in plant infection and altered endocytosis (Fig. 8B, C). This indicates that both the S/TKc domain and the RPTAPPKP motif are essential for the role of MoArk1 in endocytosis and virulence.

DISCUSSION

Endocytosis is the process by which eukaryotic cells internalize macromolecules containing plasma membrane lipids and associated proteins in vesicles that fuse with the endosomal system. Subsequent sorting into different endosomal domains determines whether a given cargo recycles to the plasma membrane, traffics to the Golgi or follows the endocytic pathway to the vacuolar lumen, undergoing degradation (Penalva, 2010). *Saccharomyces cerevisiae* has played a key role in our understanding of the endocytic internalization process, and ScArk1p is one of the proteins that regulates endocytosis through binding to other cortical actin cytoskeleton proteins. As a serine/threonine kinase, ScArk1p initiates phosphorylation cycles that control the endocytic machinery (Galletta and Copper, 2009). Here, we characterized *MoARK1*, a ScArk1 homologue from *M. oryzae*, and found that it too plays a role in the regulation of endocytosis and the actin cytoskeleton. We confirmed that such important functions endow MoArk1 with a role in growth, cell wall integrity and virulence.

MoArk1 plays a role in the cell wall integrity of *M. oryzae*

In *M. oryzae*, the cell wall undergoes considerable changes during morphogenesis (Jeon *et al*., 2008). Previous studies have revealed

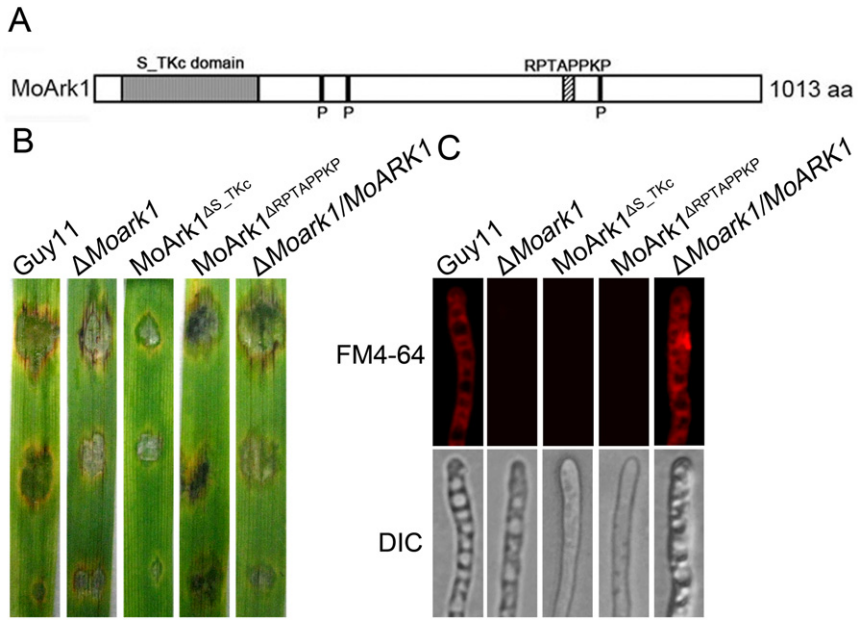

Fig. 8 Function of serine/threonine kinase (S/TKc) domain and RPTAPPKP motif. (A) Prediction domains of MoArk1. (B) Pathogenicity of mutants MoArk1$^{\Delta S/TKc}$ and MoArk1$^{\Delta RPTAPPKP}$. (C) FM4-64 staining of mutants MoArk1$^{\Delta S/TKc}$ and MoArk1$^{\Delta RPTAPPKP}$ revealed that they were defective in endocytosis. DIC, differential interference contrast image.

that most cell wall-defective mutants with breached cell wall integrity exhibit various developmental defects and are nonpathogenic (Jeon *et al*., 2008; Li *et al*., 2006). In addition, the polarized growth of filamentous fungi has been speculated to require the endocytic uptake and recycling of cell wall components, such as chitin (Harris, 2006). Multiple signalling pathways allow organisms to respond to different extracellular stimuli and to adjust their cellular machinery according to changes in their environment. Sensing changes in environmental osmolarity is vital for cell survival. Several cell wall integrity-associated genes, such as *MoMCK1*, *MoPDEH* and *MoRGS1*, have been characterized in *M. oryzae* (Jeon *et al*., 2008; Zhang *et al*., 2011a, b), which have been described as being essential for cell wall integrity and pathogenicity. Consistent with these studies, we found that the weakened cell walls and membranes were coupled with the abnormal distribution of chitins in the Δ*Moark1* mutants. Thus, the disruption of normal membrane trafficking by MoArk1 may negatively affect the secretory transport of chitosomes containing chitins and the enzymes that synthesize chitin. Meanwhile, the Δ*Moark1* mutant exhibited some resistance to cell wall stress-inducing agents, such as CFW, at higher concentrations, which may result from changes in cell wall metabolism/composition or compensatory function by other serine/threonine kinases.

MoSec22 and MoVam7 are SNARE homologues in *M. oryzae* (Dou *et al*., 2011; Song *et al*., 2010). Targeted deletion of MoSec22 and MoVam7 resulted in numerous developmental defects, including cell wall integrity, which were very similar to the ecology phenotype of the Δ*Moark1* mutants. Thus, endocytosis signalling may exhibit cross-talk with mitogen-activated protein kinase (MAPK) signalling in the regulation of cell wall integrity. In *A. oryzae*, the homologue of *S. cerevisiae* End4/Sla2 is AoEnd4. Hyphae grown under *AoEND4*-repressed conditions displayed marked growth defects and irregularly shaped colonies as a result of apical growth defects, endocytic defects in FM4-64 and abnormal cell wall synthesis. CFW staining revealed that chitin accumulated in aberrant invagination structures under *AoEND4*-repressed conditions (Higuchi *et al*., 2009). These results suggest that proteins involved in cell wall synthesis, such as chitin synthases, are probably not recycled to the tip region and therefore accumulate in the aberrant invagination structures. Overall, this is consistent with the crucial role of endocytosis in the physiology of hyphal growth and the maintenance of cell wall integrity.

Effects of MoArk1 in endocytosis and pathogenicity

Studies in *S. cerevisiae* have demonstrated the importance of intracellular transport in the growth and differentiation of lower eukaryotic organisms. As secretory properties, in particular, have the propensity to be linked to virulence, intracellular transport in medically important pathogenic fungi, such as *Candida albicans* and *Cryptococcus neoformans*, has been the focus of several studies (Chaffin *et al*., 1998). In *C. neoformans*, deletion of the endocytic protein Cin1 resulted in mutant strains with reduced pathogenicity and pleiotropic defects, including reduced melanin production (Shen *et al*., 2010). In *M. oryzae*, defects in cell wall composition can influence appressorium formation and impair the successful infection of rice (Skamnioti *et al*., 2007). During hyphal growth and appressorium formation, endocytic markers were actively internalized by both conidia and conidial germlings on rice leaves, suggesting that endocytosis might play a major role in spore germination and growth of the germ tube.

FM4-64 staining revealed that endocytosis was blocked by the disruption of *MoARK1*, and the Δ*Moark1* mutants also failed to display the Spitzenkörper body, the structure associated with rapidly growing hyphal tips in filamentous fungi. Meanwhile, the Δ*Moark1* mutant showed infection defects on plants. During the extreme polarized growth of fungal hyphae, secretory vesicles are thought to accumulate in a subapical region called the Spitzenkörper. In Δ*Moark1* mutants, the secretory vesicles and endosome may have failed to accumulate because of the lack of the Spitzenkörper body, as well as abnormal appressorium formation, which is a terminal cell required for the penetration of the host that is formed from the germ tube tip. This indicates that growth and differentiation were compromised in the Δ*Moark1* mutants, which would probably have reduced pathogenicity on host plants as a result of a loss of endocytosis and abnormal appressoria.

The balance between endocytosis and exocytosis in *M. oryzae*

The apical recycling model predicts that a balance between exocytic and endocytic processes must be present at the hyphal tip to allow for growth and, when exocytosis and endocytosis are in balance, the resulting cell shape is a hypha (Shaw *et al*., 2011). Accordingly, the conidium shape of the Δ*Moark1* mutants displayed abnormal morphology, indicating that exocytosis and endocytosis may function in overlapping, but distinct, pathways that regulate the intracellular trafficking in *M. oryzae*. When endocytosis was down-regulated or abolished, as in the *slaB*, *fimA* and *arfB* mutants in *Aspergillus*, the cell was unable to maintain polarity (Hervas-Aguilar and Penalva, 2010; Lee *et al*., 2008; Upadhyay and Shaw, 2008). In contrast, when endocytosis was unaffected, actin patches were present at the cell apex, and hyphal growth ceased as the polarization machinery was cycled back into the cell. As a precise balance between exocytosis and endocytosis exists at the hyphal tip, one can further predict that the fungal cell could alter this balance to undergo morphogenetic changes. In *M. oryzae*, both the Δ*Movam7* and the Δ*Mosec22* mutants are defective in conidiogenesis and appressorium formation; they failed to colonize plant tissue and were unable to form conidiophores, suggesting that vesicular trafficking mediated by different SNAREs is dependent on the stage of conidiogenesis. Meanwhile, the SNARE proteins MoVam7 and MoSec22 are involved in the subcellular localization of MoArk1. Future studies on the intracellular trafficking of the endocytic pathway and the balance between endocytosis and exocytosis are warranted.

In summary, we found that MoArk1 is a multifunctional protein required for conidiogenesis and pathogenicity in *M. oryzae*. MoArk1 participates in the maintenance of cell wall integrity and intracellular trafficking. Although the precise role of MoArk1 in the regulation of endocytosis remains the subject of future studies, the multifunction of MoArk1 underscores the importance of endocytic proteins in the physiology and pathogenicity of fungi. Further studies to dissect the proteins that interact with MoArk1 and to delineate the significance of these interactions will reveal the importance of endocytosis in virulence mechanisms of *M. oryzae*.

EXPERIMENTAL PROCEDURES

Strains and culture conditions

Magnaporthe oryzae strain Guy11 was used as the parental strain, and all of the strains were cultured on CM at 28 °C unless stated otherwise. Liquid CM was used to prepare the mycelia for DNA and RNA extraction. For conidiation, strain blocks were maintained on SDC (100 g of straw, 40 g of corn powder, 15 g of agar in 1 L of distilled water) at 28 °C for 7 days in the dark, followed by 3 days of continuous illumination under fluorescent light. For medium containing cell wall-perturbing agents, the final concentrations were 0.005, 0.01 and 0.02% for SDS, 200, 400 and 600 μg/mL for CR, and 200, 400 and 600 μg/mL for CFW.

MoARK1 cloning and sequence analysis

A full-length cDNA fragment for the *MoARK1* gene was isolated from the Guy11 strain. cDNA was cloned into the pMD19 T-vector (TaKaRa, Dalian, China) to generate pMD-*MoARK1* and verified by sequencing. Amino acid sequence alignments were performed using the CLUSTAL_W program and the calculated phylogenetic tree was viewed using the Mega3.1 Beta program.

Disruption of *MoARK1* and Δ*Moark1* mutant complementation

The vector pMD-*MoARK1* was constructed for targeted gene deletion by inserting the hygromycin resistance *HPH* marker gene cassette into the two flanking sequences of the *MoARK1* gene (Fig. S2A). A 1.0-kb upstream flanking sequence and a 1.1-kb downstream flanking sequence were amplified with the primer pairs FL8678/FL8679 and FL8680/FL8681, respectively. Two PCR fragments were linked by overlap PCR with primer pair FL8678/FL8681, and the linked sequence was cloned into the pMD19 T-vector. The *HPH* gene cassette, amplified with primers FL1111/FL1112, was inserted into pMD-*MoARK1* at the *Pme*I site to generate the final pMD-*MoARK1*KO. A 3.5-kb fragment containing the *MoARK1* disruption allele was amplified using primers FL8678/FL8681, purified and used to transform Guy11 according to established protocols. Table S1 (see Supporting Information) lists all of the primers used.

Putative Δ*Moark1* mutants were screened by PCR and confirmed by Southern blotting analysis (Fig. S2B, C). Further confirmation was performed through RT-PCR with primers FL8682/FL8683. For complementation, a 4.9-kb PCR product containing the full-length *MoARK1* coding region and the 1.5-kb upstream region, was amplified using primers FL9653/FL9654 and subcloned into pYF11, generating pYF11-*MoARK1R*. The resulting transformants were first screened by phenotype characterization, followed by PCR amplification, and verified by fully restored growth.

Assays for dry weight, protoplast release, vegetative growth, conidiation and appressorium formation

For vegetative growth, mycelial plugs of 3 mm × 3 mm were transferred from 7-day-old CM plates and inoculated onto fresh media (CM, V8, OM and SDC) (Zhang *et al*., 2010), followed by incubation at 28 °C. The radial growth was measured after incubation for 6 days. All experiments were repeated three times, each with three replicates. For conidia production, mycelia were grown in the dark on SDC medium at 28 °C for 7 days, followed by constant illumination for 3–4 days. Conidia were collected by washing with double-distilled water (ddH_2O), filtered through three-layer lens paper and concentrated by centrifugation (6000 ***g***) for 10 min. The final spores were suspended in 2 mL of ddH_2O and counted using a haemacytometer.

Appressorium formation was measured on Gel Bond film (FMC Bioproducts, Rockland, ME, USA), as described previously (Zhang *et al*., 2011c). Appressoria were observed through direct microscopic examination and percentages were obtained from at least 100 conidia per replicate at 24 and 48 h in at least three experiments.

Light microscopy studies

To examine hyphal morphology, strains were grown on a thin layer of CM agar on the microscope slides. After 2 days in a 28 °C growth chamber, the hyphae were observed under an Olympus BH-2 microscope (Olympus, Tokyo, Japan). The cell wall, hyphal septum and conidia were visualized by CFW (10 μg/mL, Sigma, St. Louis, MO, USA) staining, as described by Harris *et al*. (1994). FM4-64 staining was conducted following the procedures described previously (Fischer-Parton *et al*., 2000). Fluorescence microscopy was performed using laser scanning confocal microscopy.

Pathogenicity assay

Conidia were harvested from 10-day-old SDC agar cultures, filtered through three layers of lens paper and resuspended to a concentration of 5×10^4 spores/mL in a 0.2% (w/v) gelatin solution. For the detached leaf assay, leaves from 7-day-old barley (cv. Four-arris) seedlings were used. Two-week-old seedlings of rice (*Oryza sativa* cv. CO39) and 7-day-old seedlings of barley were used for infection assays. Three 20-μL droplets were placed onto the upper side of the barley leaves maintained on 4% (w/v) water agar (WA) plates. Photographs were taken 5 days after incubation at 25 °C. For spray inoculation, 5 mL of a conidial suspension of each treatment were sprayed onto rice with a sprayer. Inoculated plants were kept in a growth chamber at 25 °C with 90% humidity and in the dark for the first 24 h, followed by a 12 h/12 h light/dark cycle. Lesion formation was observed daily and photographed 7 days after inoculation (Guo *et al*., 2011).

Measurement of the chitin content

The chitin (*N*-acetylglucosamine, GlcNAc) content was determined as described by Bulik *et al*. (2003). Briefly, for each sample, 5 mg of freeze–dried mycelia were resuspended in 1 mL of 6% KOH and heated at 80 °C for 90 min. Samples were centrifuged (16 000 ***g***, 10 min) and the pellets were washed with phosphate-buffered saline in three cycles of centrifugation and suspension (16 000 ***g***, 10 min), before final suspension in 0.5 mL of McIlvaine's buffer (pH 6). An aliquot of 100 μL (13 units) of *Streptomyces plicatus* chitinase (Sigma) was added and incubation was carried out for 16 h at 37 °C with gentle mixing; 100-μL samples were then combined with 100 μL of 0.27 M sodium borate (pH 9), heated for 10 min at 100 °C, and 1 mL of freshly diluted (1:10) Ehrlich's reagent (10 g *p*-dimethylaminobenzaldehyde in 1.25 mL of HCl and 8.75 mL of glacial acetic acid) was added. After incubation at 37 °C for 20 min, 1 mL of the sample was transferred to a 2.5-mL plastic cuvette (Greiner, Bahlingen, Germany) and the absorbance at 585 nm was recorded. Standard curves were prepared with GlcNAc (Sigma). The experiment was repeated three times.

ACKNOWLEDGEMENTS

This research was supported by the National Basic Research Program of China (Grant No: 2012CB114000 to ZZ), Natural Science Foundation of China (Grant No: 31271998 to ZZ, 30971890 to XZ), the Fundamental Research Funds for the Central Universities (Grant No: KYZ201105 to ZZ) and the Project of Jiangsu of China (Grant No: Sx (2009) 54 to XZ). Research in Ping Wang's laboratory was supported by US grants (NIH/NIAID AI054958 and AI074001).

REFERENCES

Atkinson, H.A., Daniels, A. and Read, N.D. (2002) Live-cell imaging of endocytosis during conidial germination in the rice blast fungus, *Magnaporthe grisea*. *Fungal Genet. Biol.* **37**, 233–244.

Bulik, D.A., Olczak, M., Lucero, H.A., Osmond, B.C., Robbins, P.W. and Specht, C.A. (2003) Chitin synthesis in *Saccharomyces cerevisiae* in response to supplementation of growth medium with glucosamine and cell wall stress. *Eukaryot. Cell*, **2**, 886–900.

Chaffin, W.L., Lopez-Ribot, J.L., Casanova, M., Gozalbo, D. and Martinez, J.P. (1998) Cell wall and secreted proteins of *Candida albicans*: identification, function, and expression. *Microbiol. Mol. Biol. Rev.* **62**, 130–180.

Cope, M.J., Yang, S., Shang, C. and Drubin, D.G. (1999) Novel protein kinases Ark1p and Prk1p associate with and regulate the cortical actin cytoskeleton in budding yeast. *J. Cell Biol.* **144**, 1203–1218.

Davis, N.G., Horecka, J.L. and Sprague, G.F. Jr (1993) Cis- and trans-acting functions required for endocytosis of the yeast pheromone receptors. *J. Cell Biol.* **122**, 53–65.

DeJong, J.C., MCCormack, B.J., Smirnoff, N. and Talbot, N.J. (1997) Glycerol generates turgor in rice blast. *Nature*, **389**, 244–245.

D'Hondt, K., Heese-Peck, A. and Riezman, H. (2000) Protein and lipid requirements for endocytosis. *Annu. Rev. Genet.* **34**, 255–295.

Dou, X.Y., Wang, Q., Qi, Z.Q., Song, W.W., Wang, W., Guo, M., Zhang, H.F., Zhang, Z.G., Wang, P. and Zheng, X.B. (2011) MoVam7, a conserved SNARE involved in vacuole assembly, is required for growth, endocytosis, ROS accumulation, and pathogenesis of *Magnaporthe oryzae*. *PLoS ONE*, **6**, e16439.

Emans, N., Zimmermann, S. and Fischer, R. (2002) Uptake of a fluorescent marker in plant cells is sensitive to brefeldin A and wortmannin. *Plant Cell*, **14**, 71–86.

Fischer-Parton, S., Parton, R.M., Hickey, P.C., Dijksterhuis, J., Atkinson, H.A. and Read, N.D. (2000) Confocal microscopy of FM4-64 as a tool for analysing endocytosis and vesicle trafficking in living fungal hyphae. *J. Microsc. Oxf.* **198**, 246–259.

Fuchs, U. and Steinberg, G. (2005) Endocytosis in the plant-pathogenic fungus *Ustilago maydis*. *Protoplasma*, **226**, 75–80.

Fuchs, U., Hause, G., Schuchardt, I. and Steinberg, G. (2006) Endocytosis is essential for pathogenic development in the corn smut fungus *Ustilago maydis*. *Plant Cell*, **18**, 2066–2081.

Fukuda, R., McNew, J.A., Weber, T., Parlati, F., Engel, T., Nickel, W., Rothman, J.E. and Sollner, T.H. (2000) Functional architecture of an intracellular membrane t-SNARE. *Nature*, **407**, 198–202.

Galletta, B.J. and Cooper, J.A. (2009) Actin and endocytosis: mechanisms and phylogeny. *Curr. Opin. Cell Biol.* **21**, 20–27.

Gow, N.A.R., Brown, A.J.P. and Odds, F.C. (2002) Fungal morphogenesis and host invasion. *Curr. Opin. Microbiol.* **5**, 366–371.

Guo, M., Guo, W., Chen, Y., Dong, S.M., Zhang, X.B., Zhang, H.F., Song, W.W., Wang, W., Lv, R.L., Zhang, Z.G., Wang, Y.C. and Zheng, X.B. (2010) The basic leucine zipper transcription factor Moatf1 mediates oxidative stress responses and is necessary for full virulence of the rice blast fungus *Magnaporthe oryzae*. *Mol. Plant–Microbe Interact.* **23**, 1053–1068.

Guo, M., Chen, Y., Du, Y., Dong, Y.H., Guo, W., Zhai, S., Zhang, H.F., Dong, S.M., Zhang, Z.G., Wang, Y.C., Wang, P. and Zheng, X.B. (2011) The bZIP transcription factor MoAP1 mediates the oxidative stress response and is critical for pathogenicity of the rice blast fungus *Magnaporthe oryzae*. *PLoS Pathog.* **7**, e1001302.

Harris, S.D. (2006) Cell polarity in filamentous fungi: shaping the mold. *Int. Rev. Cytol.* **251**, 41–77.

Harris, S.D., Morrell, J.L. and Hamer, J.E. (1994) Identification and characterization of *Aspergillus nidulans* mutants defective in cytokinesis. *Genetics*, **136**, 517–532.

Harris, S.D., Read, N.D., Roberson, R.W., Shaw, B., Seiler, S., Plamann, M. and Momany, M. (2005) Polarisome meets Spitzenkörper: microscopy, genetics, and genomics converge. *Eukaryot. Cell*, **4**, 225–229.

Heath, I.B., Bonham, M., Akram, A. and Gupta, G.D. (2003) The interrelationships of actin and hyphal tip growth in the ascomycete *Geotrichum candidum*. *Fungal Genet. Biol.* **38**, 85–97.

Hervas-Aguilar, A. and Penalva, M.A. (2010) Endocytic machinery protein SlaB is dispensable for polarity establishment but necessary for polarity maintenance in hyphal tip cells of *Aspergillus nidulans*. *Eukaryot. Cell*, **9**, 1504–1518.

Higuchi, Y., Shoji, J.Y., Arioka, M. and Kitamoto, K. (2009) Endocytosis is crucial for cell polarity and apical membrane recycling in the filamentous fungus *Aspergillus oryzae*. *Eukaryot. Cell*, **8**, 37–46.

Howard, R.J. and Valent, B. (1996) Breaking and entering: host penetration by the fungal rice blast pathogen *Magnaporthe grisea*. *Annu. Rev. Microbiol.* **50**, 491–512.

Idrissi, F.Z., Grotsch, H., Fernandez-Golbano, I.M., Presciatto-Baschong, C., Riezman, H. and Geli, M.I. (2008) Distinct acto/myosin-I structures associate with endocytic profiles at the plasma membrane. *J. Cell Biol.* **180**, 1219–1232.

Jeon, J., Goh, J., Yoo, S., Chi, M.H., Choi, J., Rho, H.S., Park, J., Han, S.S., Kim, B.R., Park, S.Y., Kim, S. and Lee, Y.H. (2008) A putative MAP kinase kinase kinase, MCK1, is required for cell wall integrity and pathogenicity of the rice blast fungus, *Magnaporthe oryzae*. *Mol. Plant–Microbe Interact.* **21**, 525–534.

Kaksonen, M., Sun, Y. and Drubin, D.G. (2003) A pathway for association of receptors, adaptors, and actin during endocytic internalization. *Cell*, **115**, 475–487.

Kaksonen, M., Toret, C.P. and Drubin, D.G. (2006) Harnessing actin dynamics for clathrin-mediated endocytosis. *Nat. Rev. Mol. Cell Biol.* **7**, 404–414.

Kim, J.H., Kim, H.W., Heo, D.H., Chang, M., Baek, I.J. and Yun, C.W. (2009) FgEnd1 is a putative component of the endocytic machinery and mediates ferrichrome uptake in *Fusarium graminearum*. *Curr. Genet.* **55**, 593–600.

Lee, K., Singh, P., Chung, W.C., Ash, J., Kim, T.S., Hang, L. and Park, S. (2006) Light regulation of asexual development in the rice blast fungus, *Magnaporthe oryzae*. *Fungal Genet. Biol.* **43**, 694–706.

Lee, S.C., Schmidtke, S.N., Dangott, L.J. and Shaw, B.D. (2008) *Aspergillus nidulans* ArfB plays a role in endocytosis and polarized growth. *Eukaryot. Cell*, **7**, 1278–1288.

Li, S.J., Myung, K., Guse, D., Donkin, B., Proctor, R.H., Grayburn, W.S. and Calvo, A.M. (2006) FvVE1 regulates filamentous growth, the ratio of microconidia to macroconidia and cell wall formation in *Fusarium verticillioides*. *Mol. Microbiol.* **62**, 1418–1432.

Pelham, H.R. (1999) SNAREs and the secretory pathway—lessons from yeast. *Exp. Cell Res.* **247**, 1–8.

Penalva, M.A. (2010) Endocytosis in filamentous fungi: Cinderella gets her reward. *Curr. Opin. Microbiol.* **13**, 684–692.

Raths, S., Rohrer, J., Crausaz, F. and Riezman, H. (1993) end3 and end4: two mutants defective in receptor-mediated and fluid-phase endocytosis in *Saccharomyces cerevisiae*. *J. Cell Biol.* **120**, 55–65.

Read, N.D. and Kalkman, E.R. (2003) Does endocytosis occur in fungal hyphae? *Fungal Genet. Biol.* **39**, 199–203.

Shaw, B.D., Chung, D.W., Wang, C.L., Quintanilla, L.A. and Upadhyay, S. (2011) A role for endocytic recycling in hyphal growth. *Fungal. Biol.* **115**, 541–546.

Shen, G., Whittington, A., Song, K. and Wang, P. (2010) Pleiotropic function of intersectin homologue Cin1 in Cryptococcus neoformans. *Mol. Microbiol.*, **76**, 662–676.

Skamnioti, P., Henderson, C., Zhang, Z., Robinson, Z. and Gurr, S.J. (2007) A novel role for catalase B in the maintenance of fungal cell-wall integrity during host invasion in the rice blast fungus *Magnaporthe grisea*. *Mol. Plant–Microbe Interact.* **20**, 568–580.

Smythe, E. and Ayscough, K.R. (2003) The Ark1/Prk1 family of protein kinases. Regulators of endocytosis and the actin skeleton. In: *EMBO Rep.* **4**, 246–251.

Song, W.W., Dou, X.Y., Qi, Z.Q., Wang, Q., Zhang, X., Zhang, H.F., Guo, M., Dong, S.M., Zhang, Z.G., Wang, P. and Zheng, X.B. (2010) R-SNARE homolog MoSec22 is required for conidiogenesis, cell wall integrity, and pathogenesis of *Magnaporthe oryzae*. *PLoS ONE*, **5**, e13193.

Steinberg, G. (2007) On the move: endosomes in fungal growth and pathogenicity. *Nat. Rev. Microbiol.* **5**, 309–316.

Talbot, N.J. and Foster, A.J. (2001) Genetics and genomics of the rice blast fungus *Magnaporthe grisea*: developing an experimental model for understanding fungal diseases of cereals. *Adv. Bot. Res.* **34**, 263–287.

Thines, E., Weber, R.W. and Talbot, N.J. (2000) MAP kinase and protein kinase A-dependent mobilization of triacylglycerol and glycogen during appressorium turgor generation by *Magnaporthe grisea*. *Plant Cell*, **12**, 1703–1718.

Toret, C.P. and Drubin, D.G. (2006) The budding yeast endocytic pathway. *J. Cell Sci.* **119**, 4585–4587.

Upadhyay, S. and Shaw, B.D. (2008) The role of actin, fimbrin and endocytosis in growth of hyphae in *Aspergillus nidulans*. *Mol. Microbiol.* **68**, 690–705.

Valent, B., Farrall, L. and Chumley, F.G. (1991) *Magnaporthe grisea* genes for pathogenicity and virulence identified through a series of backcrosses. *Genetics*, **127**, 87–101.

Verdin, J., Bartnicki-Garcia, S. and Riquelme, M. (2009) Functional stratification of the Spitzenkörper of *Neurospora crassa*. *Mol. Microbiol.* **74**, 1044–1053.

Virag, A. and Harris, S.D. (2006) The Spitzenkörper: a molecular perspective. *Mycol. Res.* **110**, 4–13.

Wang, P. and Shen, G. (2011) The endocytic adaptor proteins of pathogenic fungi: charting new and familiar pathways. *Med. Mycol.* **49**, 449–457.

Zhang, H.F., Liu, K.Y., Zhang, X., Song, W.W., Zhao, Q., Dong, Y.H., Guo, M., Zheng, X.B. and Zhang, Z.G. (2010) A two-component histidine kinase, MoSLN1, is required for cell wall integrity and pathogenicity of the rice blast fungus, *Magnaporthe oryzae*. *Curr. Genet.* **56**, 517–528.

Zhang, H.F., Liu, K.Y., Zhang, X., Tang, W., Wang, J.S., Guo, M., Zhao, Q., Zheng, X.B., Wang, P. and Zhang, Z.G. (2011a) Two phosphodiesterase genes, PDEL and PDEH, regulate development and pathogenicity by modulating intracellular cyclic AMP levels in *Magnaporthe oryzae*. *PLoS ONE*, **6**, e17241.

Zhang, H.F., Tang, W., Liu, K.Y., Huang, Q., Zhang, X., Yan, X., Chen, Y., Wang, J.S., Qi, Z.Q., Wang, Z.Y., Zheng, X.B., Wang, P. and Zhang, Z.G. (2011b) Eight RGS and RGS-like proteins orchestrate growth, differentiation, and pathogenicity of *Magnaporthe oryzae*. *PLoS Pathog.* **7**, e1002450.

Zhang, L.S., Lv, R.L., Dou, X.Y., Qi, Z.Q., Hua, C.L., Zhang, H.F., Wang, Z.Y., Zheng, X.B. and Zhang, Z.G. (2011c) The function of MoGlk1 in integration of glucose and ammonium utilization in *Magnaporthe oryzae*. *PLoS ONE*, **6**, e22809.

SUPPORTING INFORMATION

Additional Supporting Information may be found in the online version of this article at the publisher's web-site:

Fig. S1 *Magnaporthe oryzae* MoArk1 is a fungal actin-regulating kinase 1 (Ark1) protein. (A) Prediction of domains of MoArk1 using the SMART website. (B) Phylogenetic analysis of MoArk1 and other Ark1 homologues, including MoArk1 (*Magnaporthe oryzae*, XP_003713889.1), *Neurospora crassa* (XP_962918.1), *Fusarium graminearum* (EGU75522.17), *Aspergillus nidulans* (XP_661798.1), *Saccharomyces cerevisiae* (NP_014378.1), *Saccharomyces cerevisiae* (NP_012171.1), *Candida albicans* (XP_446476.1), *Ustilago maydis* (XP_759228.1) and *Saccharomyces cerevisiae* (NP_009615.1). Sequence alignments were performed using the CLUSTAL_W program, and the calculated phylogenetic tree was viewed using the Mega3.1 Beta program.

Neighbour-joining tree with 1000 bootstrap replicates of phylogenetic relationships among fungal Ark1 homologues. Numbers above the branches represent amino acid substitution.

Fig. S2 Targeted gene replacement and complementation. (A) Restriction map of the *MoARK1* genomic region. Disruption construct containing the homologous sequences flanking the *HPH* cassette to replace a part of *MoARK1*. (B) Expression analysis of *MoARK1* in the wild-type, Δ*Moark1* mutant and complemented strains using *Actin* as a control. (C) Southern blot analysis of the Δ*Moark1* mutant (lanes 1 and 2) and the wild-type (lane 3) strains using *MoARK1*- or *HPH*-specific probes. Genomic DNA was digested with *Eco*RI.

Fig. S3 Assessment of tolerance to salt and osmotic stresses. (A) The Δ*Moark1* mutant, wild-type and complemented strains were incubated on complete medium (CM) plates containing KCl, NaCl and sorbitol at various concentrations at 28 °C for 7 days. (B) Colony inhibition rate measurement. Inhibition rate = [(diameter of untreated strain—diameter of treated strain)/diameter of untreated strain] × 100%. Error bars represent the standard deviations and asterisks indicate a significant difference between the mutants and wild-type strain at $P < 0.05$, according to Duncan's range test.

Fig. S4 Responses of wild-type, Δ*Moark1* and Δ*Moark1/MoARK1* strains to cell wall-disturbing agents. (A, C) The Δ*Moark1* mutant, wild-type and complemented strains were incubated on complete medium (CM) plates supplemented with various stress inducers for 7 days at 28 °C. (B, D, E) Statistical analysis of the growth inhibition rate of mycelia on CM supplemented with cell wall-disturbing agents. Double asterisks indicate a significant difference between the mutants and wild-type strain at $P < 0.01$, and single asterisk indicates a significant difference at $P < 0.05$.

Fig. S5 *MoARK1* is related to tolerance to H_2O_2 and the activity of extracellular peroxidase. (A) Δ*Moark1* mutants were less sensitive to a higher concentration of H_2O_2. The Guy11, Δ*Moark1* mutants and complemented strain were incubated on complete medium (CM) plates supplemented with 2.5 and 5 mM H_2O_2 for 6 days before being photographed. (B) Statistical analysis of the growth inhibition rate of mycelial growth on CM supplemented with H_2O_2. Asterisks indicate a significant difference between the mutants and wild-type strain at $P < 0.01$, according to Duncan's range test. (C) The discoloration of Congo Red was tested on CM plates containing 200 μg/mL of the dye at a final concentration. Discoloration was observed on day 7 after inoculation at 28 °C. (D) Peroxidase activity was measured using the ABTS oxidizing test under normal and H_2O_2-supplemented conditions. (E) Expression profiles of five genes encoding predicted peroxidases under normal or oxidative stress-induced conditions.

Table S1 Primers used in this study.